

Improvement of the ACI method for calculation of deflections of reinforced concrete beams

Melhoramento do método do ACI para o cálculo de flechas de vigas de concreto armado

José Milton de Araújo

Departamento de Materiais e Construção – FURG – Rio Grande, RS

e-mail: ed.dunas@mikrus.com.br

ABSTRACT: The simplified method of ACI for prediction of deflections of reinforced concrete beams is analyzed in this work. Results obtained with this method are compared with those obtained through a nonlinear analysis. Additional deflections due to creep and shrinkage are considered in the study. The results indicate that the ACI method is appropriate for calculation of instantaneous deflections of reinforced concrete beams. However, this method is not satisfactory for evaluation of long-term deflections of reinforced concrete beams. Some modifications are suggested to improve the accuracy of the simplified method.

RESUMO: Neste trabalho analisa-se o método simplificado do ACI para o cálculo de flechas em vigas de concreto armado. Os resultados obtidos com esse método são comparados com os resultados de uma análise não-linear. As flechas adicionais devidas à fluência e à retração são consideradas no estudo. Os resultados indicam que o método do ACI é satisfatório para o cálculo das flechas iniciais das vigas de concreto armado. Entretanto, esse método não é adequado para a avaliação das flechas de longa duração das vigas de concreto armado. Algumas modificações são sugeridas para melhorar o método simplificado.

1. INTRODUCTION

Present design procedures of reinforced concrete structures are based on limit states concepts. They are generally classified as ultimate limit states and serviceability limit states.

The ultimate limit state refers to the bearing capacity of a structural part or of the structure as a whole. In this phase of the design procedures, attention is given to the criteria for structural resistance. Actions and sectional efforts are evaluated and partial safety factors are introduced to obtain a target reliability level.

The serviceability limit states are associated with the structural performance under expected actions in normal conditions of utilization. It is generally necessary to consider two limit states: the limit state of cracking and the limit state of deformation. Other serviceability limit states, such as excessive vibration, may be necessary to consider when dynamic actions are present.

In the verifications of the serviceability limit states, actions are considered with characteristic values, what is equivalent to considering partial safety factors as equal to one. In the same way, mean mechanical properties of the materials are used to evaluate the structural rigidity.

Usually, design codes for reinforced concrete structures require that beam deflections are calculated for the quasi-permanent combination of the actions. Creep and shrinkage effects should be included in this analysis.

The quasi-permanent combinations are actions that can act during great part of the useful life of the structures. In each combination, permanent action is represented by a single representative value, D . Usually, this value is considered as a mean value, which is calculated from nominal dimensions of the structural elements¹. Variable actions are considered with the quasi-permanent values $\psi_2 L$, where L is the characteristic value and $\psi_2 < 1$.

According to the CEB², for example, for the accidental loads of residential buildings and of office buildings, it is necessary to consider $\psi_2 = 0.4$. In these cases, the quasi-permanent load P_o is given by

$$P_o = D + 0.4L \quad (1)$$

where D and L are the characteristic values of the dead load and the live load, respectively.

Once the analysis is made for the service loads, it is admitted that the compression stresses in the structure are small enough so that it is possible to consider a lineal elastic behavior for concrete. Then, it is possible to elaborate simplified procedures of analysis, where the only source of nonlinearity is due to the cracking of concrete. With that, a reasonable simplification is gotten, which facilitates the reinforced concrete structural analysis.

In a consistent analysis of reinforced concrete beam, it is necessary to take into account the cracking and the tension stiffening effect. Creep and shrinkage of concrete should also be considered for calculation of long-term deflection.

The analysis may be accomplished with different refinement levels, from the nonlinear analysis, until the utilization of simplified methods as the bilinear method adopted by CEB³ and in Eurocode-2⁴.

On the other hand, the ACI Building Code⁵ recommends a simplified formula to represent the equivalent rigidity of the cracked beam. Additional long-term deflection, resulting from creep and shrinkage, is included as an extra term.

This method of ACI has been adopted in several national codes, as in EHE-99⁶ of Spain, in NBR-6118⁷ of Brazil, and in the codes of several countries all over the world.

The objective of this work is to verify the accuracy of this simplified method of ACI and to suggest some improvements. The nonlinear model presented in the following section is considered as the reference model.

2. NONLINEAR MODEL FOR REINFORCED CONCRETE BEAMS ANALYSIS

Deformations of reinforced concrete beams should be calculated considering the material nonlinearities due to concrete and steel behavior.

Then, it is necessary to adopt stress-strain relationships compatible with the experimental results obtained in uniaxial tests.

For reinforced concrete beams that are submitted to the service loads the tension stiffening effect is of fundamental importance. This behavior may be modeled through a stress-strain relationship of steel embedded in concrete^{1,8,9}. Alternatively, a stress-strain relationship for concrete in tension, including a descending branch, may also be used^{10,11,12}.

On the other hand, it is necessary to consider creep and shrinkage effects, which can be made through several rheological models^{13,14}. The use of rheological models, based on Maxwell or Kelvin chains, demands a time integration where the deformations of the structure are obtained step by step. This procedure is onerous and unnecessary in design level, especially in building design, for the following reasons:

1. The time integration leads to results that depend on the creep function.

2. The experimental results indicate a great variability in the development of creep in the course of time, so that any creep function to be adopted represents just a rough estimate of the concrete behavior.

3. The quasi-permanent loading that is used in the analysis only represents a conventional value of actual long-time loads that act in the structure.

4. The actual loading in the structure is not known and it can vary enough from one structure to another.

In view of this, the numeric analyses through rheological chains lose importance when applied to the design of building structures, though they represent with greater fidelity the concrete behavior. In these cases, it is desirable to obtain the final answer of the structure starting from entrance parameters that are estimated for loads and for properties of the materials, particularly the mechanical properties of concrete. In that way, the nonlinear model should have the balance between the numeric accuracy and the simplicity to become compatible with the reality.

The nonlinear model adopted in this work is the classic layered model which is used largely in reinforced concrete nonlinear analysis. This model had its accuracy demonstrated in previous works^{8,15} and it allows obtaining the probable deflections of reinforced concrete beams.

The stress-strain diagram for concrete subjected to compression is shown in Fig. 1.

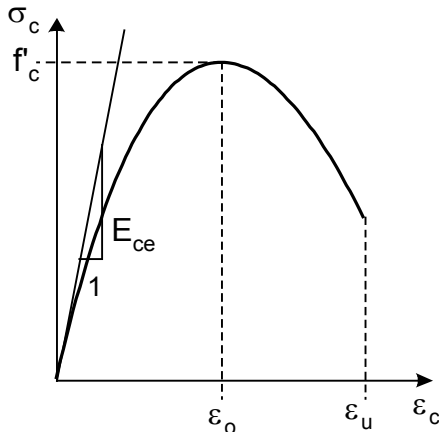


Fig. 1 – Stress-strain diagram for concrete in uniaxial compression

Several expressions have been proposed to represent the stress-strain diagram for concrete in uniaxial compression^{1,16,17}. According to CEB¹, for example, the compression stress σ_c , is given by

$$\sigma_c = -f'_c \left[\frac{k\eta - \eta^2}{1 + (k-2)\eta} \right] \quad (2)$$

where $k = -E_{ce}\epsilon_o/f'_c$; $\eta = \epsilon_c/\epsilon_o$ and ϵ_c is the compression strain.

For the strain ϵ_o , corresponding to the peak compressive stress f'_c , the value $\epsilon_o = -0.0022(1 + \varphi)$ is adopted, where φ is the creep coefficient. The ultimate strain is $\epsilon_u = -0.0035(1 + \varphi)$.

The modulus of elasticity of concrete, E_c , may be estimated from the compressive strength f'_c , using empirical relationships presented in the design codes^{1,5}.

For long-term loading, the total deformation including creep is calculated by using an effective modulus of elasticity for concrete, E_{ce} , given by

$$E_{ce} = \frac{E_c}{1 + \varphi} \quad (3)$$

For concrete subjected to tension the stress-strain diagrams indicated in Fig. 2 are adopted.

The tensile stress σ_{ct} is given by

$$\sigma_{ct} = \begin{cases} E_{ce}\epsilon_{ct}, & \text{se } \epsilon_{ct} \leq (1 + \varphi)\epsilon_{cr} \\ \sigma_{ct,lim}, & \text{se } \epsilon_{ct} > (1 + \varphi)\epsilon_{cr} \end{cases} \quad (4)$$

where ϵ_{ct} is the tensile strain and $\sigma_{ct,lim}$ is the maximum tensile stress for cracked concrete, given by

$$\sigma_{ct,lim} = f_{ct} \left(\frac{\epsilon_{cr}}{\epsilon_{ct}} \right)^{0.6} \quad (5)$$

where $\epsilon_{cr} = f_{ct}/E_c$ is the cracking strain of concrete for short-term loads.

The expression (5) takes into account the tension stiffening effects.

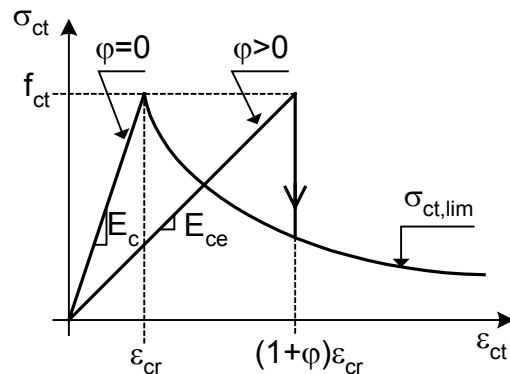


Fig. 2 – Stress-strain diagrams for concrete in tension

The axial tensile strength f_{ct} may be estimated from the compressive strength f'_c , using empirical relationships presented in the design codes^{1,5}.

As it may be observed, the constitutive model is an extension of the effective modulus method for the nonlinear case. This model is satisfactory when the history of stress is characterized by limited variations during the aging of concrete.

When great stress variations occur during the aging period, the model may be improved applying the adjusted effective modulus method^{18,19}. That is equivalent to consider an adjusted creep coefficient $\varphi_a = \zeta\varphi$, where ζ is the aging coefficient. In the practical applications $\zeta = 0.8$ may be adopted.

In this work $\zeta = 1$ is adopted because it is assumed that the quasi-permanent load doesn't vary in the course of time.

The total strain of concrete, $\epsilon_{c,tot}$, is given by

$$\varepsilon_{c,tot} = \varepsilon_{c\sigma} + \varepsilon_{cs} \quad (6)$$

where $\varepsilon_{c\sigma}$ is the stress dependent strain and ε_{cs} is the shrinkage strain.

Therefore, the stresses in the concrete may be obtained with the previous model considering the portion of the strain $\varepsilon_{c\sigma} = \varepsilon_{c,tot} - \varepsilon_{cs}$.

The stress-strain diagram for reinforcing steel is represented in Fig. 3. The same diagram is used for tension and for compression.

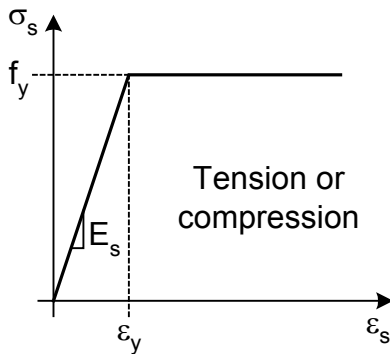


Fig. 3 – Stress-strain diagram for reinforcing steel

The structural analysis is accomplished by means of the finite element method. The finite element used is the standard element for plane frames, with two nodes and three degrees of freedom for node (one rotation and two displacements). Three Gauss integration points are considered along the finite element length, for determination of the nodal nonlinear actions.

At each integration point the concrete cross-section is discretized in $n=30$ layers in the direction of the height, as it is shown in Fig. 4. The resistant sectional forces are obtained considering the stresses in the reinforcement and in the center of each concrete layer.

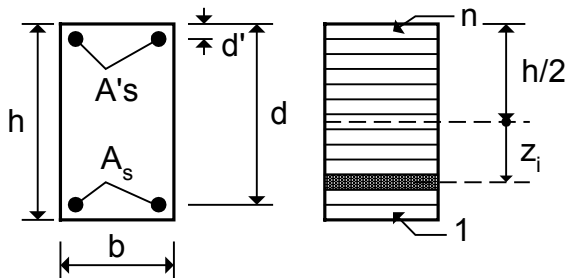


Fig. 4 – Beam cross-section and discretization in layers

Using the finite element method, the strain ε_x in a generic layer of the cross-section, located to a distance z from centroidal axis of the gross section, neglecting reinforcement, is given by

$$\varepsilon_x = \varepsilon_{x0} + z\chi \quad (7)$$

where ε_{x0} and χ represent the axial strain and the curvature, obtained through the nodal displacements of the element.

The expression (7) is also used to calculate the strain in each steel layer, being enough to use for z the distance of the steel layer to the centroidal axis of gross section. Using the stress-strain diagram of the Fig. 3, it is obtained the stress σ_s in the steel.

The expression (7) supplies the total strains in the concrete, including creep and shrinkage. The mechanical strain $\varepsilon_{c\sigma}$ is given by

$$\varepsilon_{c\sigma} = \varepsilon_{x0} + z\chi - \varepsilon_{cs} \quad (8)$$

where $z = z_i$, with $i = 1, \dots, n$, represents the distance of the center of concrete layer until the centroidal axis of gross section.

After the calculation of the strain $\varepsilon_{c\sigma}$, the constitutive model is used to obtain the stress in the center of each concrete layer.

Using the finite element method it is obtained the displacements of the structure at a desired load level. The nonlinear equations system, due to material nonlinearities, is iteratively solved using the BFGS method. Small load increments are applied on the beam until the rupture occurs.

Occurrence of the rupture is assumed when the compression strain in the concrete results smaller or equal to $\varepsilon_u = -0.0035(1 + \varphi)$, or when the tensile strain in the steel reaches the value of 0.010.

3. SIMPLIFIED METHOD OF ACI

According to ACI Building Code⁵, instantaneous deflections of reinforced concrete beams, $W(t_0)$, shall be computed with the effective moment of inertia I_e , given by

$$I_e = \left(\frac{M_{cr}}{M_a} \right)^3 I_g + \left[1 - \left(\frac{M_{cr}}{M_a} \right)^3 \right] I_{cr} \leq I_g \quad (9)$$

where

I_g = moment of inertia of gross concrete section about centroidal axis, neglecting reinforcement;

I_{cr} = moment of inertia of cracked section transformed to concrete;

M_a = maximum moment in member at stage deflection is computed;

M_{cr} = cracking moment.

The cracking moment is given by

$$M_{cr} = \frac{f_r I_g}{y_t} \quad (10)$$

where y_t is the distance from centroidal axis of the gross section, neglecting reinforcement, to extreme fiber in tension and f_r is the modulus of rupture of concrete.

Thus, for a rectangular section it results in the expression $M_{cr} = bh^2 f_r / 6$, where b is the width and h is the total height of the cross-section.

For prismatic members, effective moment of inertia I_e may be computed considering the geometrical properties of the critical section. Thus, deflections are calculated considering the effective rigidity $E_c I_e$.

Additional long-term deflection, ΔW , resulting from creep and shrinkage, is obtained by

$$\Delta W = \frac{\xi}{1 + 50\rho'} W(t_o) \quad (11)$$

where $W(t_o)$ is the instantaneous deflection caused by the sustained load and $\rho' = A'_s / (bd)$ is the compression reinforcement ratio on the critical section.

Critical section may be taken at midspan for simple and continuous beams, and at support for cantilevers.

The factor ξ depends on the duration of the load, being $\xi = 2.0$, for 5 years or more, and $\xi = 1.4$, for 12 months of duration of the load.

The total deflection of the beam, W , is given by

$$W = W(t_o) + \Delta W \quad (12)$$

Expression (9) for the effective moment of inertia was determined empirically by Branson²⁰ and it is used to consider the tension stiffening effect. Expression (11) was also obtained based on

experimental results of beams under long-term loads^{21,22}.

4. IMPROVEMENT OF THE ACI METHOD

The ACI method may be improved if the steel areas are included in the calculation of the cracking moment M_{cr} . On the other hand, when the shrinkage is included in the analysis, it is convenient to adopt the axial tensile strength f_{ct} instead of the modulus of rupture f_r to consider the unfavorable effects of the tensile stress induced by shrinkage.

Therefore, the cracking moment is obtained through the expression

$$M_{cr} = \frac{f_t I_1}{y_{1t}} \quad (13)$$

where I_1 is the moment of inertia of the uncracked transformed section, y_{1t} is the distance from centroidal axis of the transformed section to extreme fiber in tension and $f_t = f_r$, or $f_t = f_{ct}$ when the shrinkage is considered.

The values of I_1 and y_{1t} may be obtained easily, but it is convenient to simplify the calculation of the cracking moment. This may be obtained through the expression

$$M_{cr} = \frac{f_t I_g}{y_t} K_s = M_{cr,o} K_s \quad (14)$$

where the coefficient K_s depends on the tensile reinforcement ratio $\rho = A_s / (bd)$ and of the relationship $\beta = h/d$ between the total height h and the effective height d of the cross-section.

Through a regression analysis, it was found a simplified expression for K_s given by

$$K_s = 1 + (105 - 78\beta)\rho \quad (15)$$

The expression (15) was obtained for rectangular sections, but it may also be used for T-sections. In this case, $\rho = A_s / (b_w d)$, where b_w is the web width.

Fig. 5 compares the cracking moment obtained through the exact expression, given in the equation (13), and through the approximate expression,

given in the equations (14) and (15). An excellent agreement is observed between the two expressions.

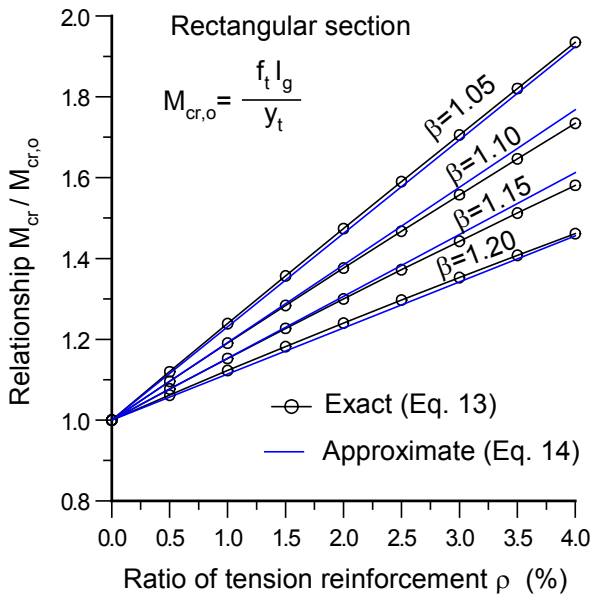


Fig. 5 – Validation of the simplified expression for the cracking moment

After the calculation of the cracking moment through the expressions (14) and (15), the effective moment of inertia I_e may be obtained by the employment of the equation (9). However, it is considered the moment of inertia I_1 of uncracked transformed section, including the reinforcement, instead of I_g .

Then, the effective moment of inertia I_e is given by

$$I_e = \left(\frac{M_{cr}}{M_a} \right)^3 I_1 + \left[1 - \left(\frac{M_{cr}}{M_a} \right)^3 \right] I_{cr} \leq I_1 \quad (16)$$

For rectangular sections, it may be written the approximate relationship

$$I_1 = \left[1 + (13\rho - 64\rho^2)(6 - 4.5\beta) \right] I_g \quad (17)$$

where β , ρ and I_g are as defined previously.

Fig. 6 compares the exact relationship I_1/I_g with the approximate relationship given in the expression (17). The exact relationship was obtained for a modular ratio $\alpha = E_s/E_c = 7.5$. As it is observed, the approach is satisfactory.

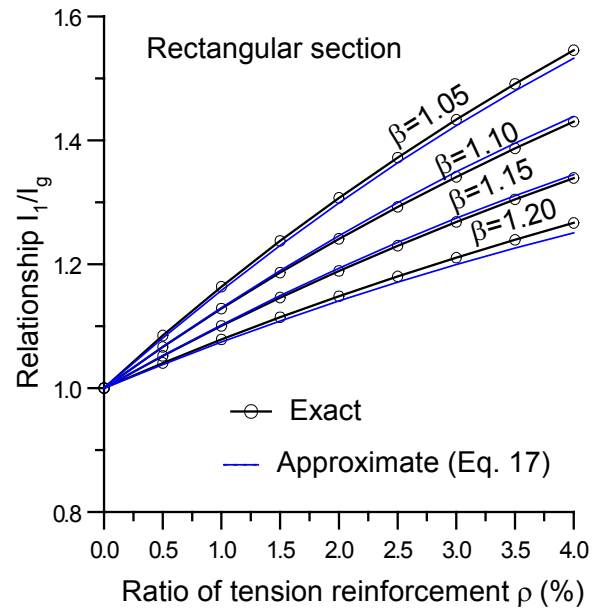


Fig. 6 – Exact and approximate relationships I_1/I_g

The moment of inertia I_{cr} for cracked rectangular sections is given by

$$I_{cr} = \left[\frac{1}{6} \lambda^2 (3 - \lambda) + \alpha \rho' (\lambda - \delta) (1 - \delta) \right] b d^3 \quad (18)$$

where

$$\lambda = -\alpha(\rho + \rho') + \sqrt{\alpha^2(\rho + \rho')^2 + 2\alpha(\rho + \delta\rho')} \quad (19)$$

with $\delta = d'/d$ according to Fig. 4.

In this version proposed for the ACI method, creep is included by using the effective modulus of elasticity for concrete according to expression (3). Thus, deflections including creep effects are calculated considering the effective stiffness $E_{ce}I_e$, where here $E_{ce} = E_c / (1 + K'_s \varphi)$. The coefficient K'_s takes into account the favorable effect of compression reinforcement in reducing long-term deflections. This coefficient is given by

$$K'_s = \frac{1}{1 + 50\rho'} \quad (20)$$

according to ACI Building Code.

The effective moment of inertia I_e is obtained through the equation (16). For the evaluation of I_{cr} it is considered the effective modular ratio $\alpha_e = (1 + K'_s \varphi) E_s / E_c$.

Shrinkage curvature χ_{cs} may be computed by expression

$$\chi_{cs} = K'_s \varepsilon_{cs} \alpha_e \frac{S_e}{I_e} \quad (21)$$

where ε_{cs} is the free shrinkage strain and S_e is the first moment of area of the reinforcement about the centroid of the equivalent section with effective moment of inertia I_e .

The centroid location of the equivalent section is ignored and its determination requires the use of an iterative process. However, the expression (22) may be used as a good approach

$$x_e = \left(\frac{M_{cr}}{M_a} \right)^3 x_1 + \left[1 - \left(\frac{M_{cr}}{M_a} \right)^3 \right] x_{cr} \leq x_1 \quad (22)$$

where

x_e = distance from extreme compression fiber to centroid of equivalent section;

x_1 = distance from extreme compression fiber to centroid of the uncracked transformed section;

x_{cr} = distance from extreme compression fiber to centroid of the fully cracked transformed section.

Equation (22) is presented by Branson²³ with the exponent of 2.5 instead of 3. However, the results differ little when either of these values is used.

The compression reinforcement may be disregarded when x_1 is calculated. Therefore, for the rectangular section shown in the Fig. 4, it results

$$x_1 = \left[\frac{\beta^2 + 2\alpha_e \rho}{2(\beta + \alpha_e \rho)} \right] d \quad (23)$$

The distance x_{cr} from extreme compression fiber to centroid of the fully cracked transformed section is $x_{cr} = \lambda d$, where λ is given in equation (19).

After the calculation of the distance x_e by using the equation (22), the first moment of area of the reinforcement S_e may be obtained. For the rectangular section of Fig. 4, it results

$$S_e = A_s (d - x_e) + A'_s (d' - x_e) \quad (24)$$

Thus, additional deflection W_{cs} resulting from shrinkage is obtained by integration of the

curvatures given in equation (21). For a single span beam, it results

$$W_{cs} = \frac{l^2}{8} \chi_{cs} \quad (25)$$

where l is the span of the beam.

Shrinkage deflection in continuous beams may be predicted by the multiplication of the deflection calculated through the equation (25) by a reduction factor. This reduction factor is 0.5 for an interior span and 0.7 for an end span¹⁸. The equation (25) may also be used for a cantilever with the coefficient 2 instead of 8.

5. EXAMPLES

The reinforced concrete single span beam of constant cross-section shown in Fig. 7 is analyzed in this work. The uniform loading is composed by the dead load D and by the live load L . In the finite element analysis, the beam span was discretized in 10 elements.

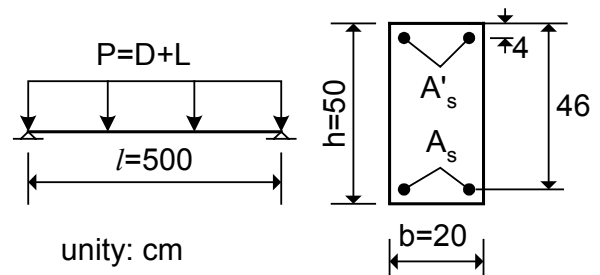


Fig. 7 – Loading and geometry of the beam

In the analyzed examples, it is assumed that the specified compressive strength of concrete is $f'_c = 25$ MPa. Using the expressions of the ACI Code, it is obtained the modulus of elasticity of concrete $E_c = 23.7$ GPa and the modulus of rupture $f_r = 3.1$ MPa. The axial tensile strength of concrete is estimated as $f_{ct} = 2.6$ MPa, according to CEB. The creep coefficient is considered equal to $\varphi = 2.5$ and free shrinkage strain is $\varepsilon_{cs} = -50 \times 10^{-5}$.

The specified yield strength of reinforcement is $f_y = 500$ MPa and it is assumed a modulus of elasticity $E_s = 200$ GPa.

The required steel areas in the beam cross-section are computed considering the strength requirements of the ACI Code. Three cases of loading are considered, as it is indicated in the

Table 1. Those values represent the service loads that usually act in the beams of the residential buildings.

The calculation of the steel area indicates that $A'_s = 0$ for the three cases of loading. Then, $A'_s = 0.62 \text{ cm}^2$ (equivalent to two bars with diameter of 6.3 mm) is adopted as compressive steel.

Table 1 indicates the loads and steel areas of the three analyzed beams.

Table 1 – Loads and steel areas of the beams

Beam	Load (kN/m)		Steel area (cm^2)	
	D	L	A_s	A'_s
A1	8.5	1.5	2.5	0.62
A2	13.0	2.0	3.4	0.62
A3	17.0	3.0	4.6	0.62

6. RESULTS

The answers of the three beams, obtained with the nonlinear model, with the ACI method and with the improved method of ACI as proposed, are shown in Fig. 8 to 10. These figures indicate the relationships between the uniform load and the midspan instantaneous deflection.

It may be observed in Fig. 8 to 10 that there is a good agreement among the three methods in all the stages of the loading. Usually, the proposed model agrees better with the nonlinear model as a consequence of the consideration of tensile reinforcement for calculation of the cracking moment. However, the influence of the reinforcement is not very significant because the reinforcement ratio is small in the three beams.

Table 2 indicates the values of the instantaneous deflection for the total service load $D+L$. As it is observed, the proposed model agrees better with the nonlinear analysis than the method of ACI.

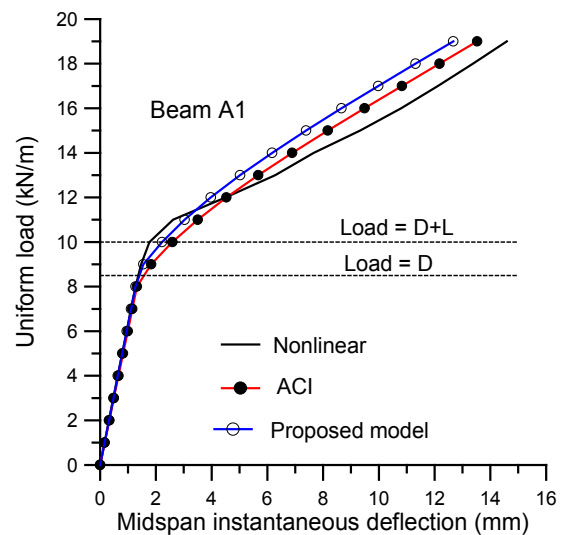


Fig. 8 – Load-instantaneous deflection curves for beam A1

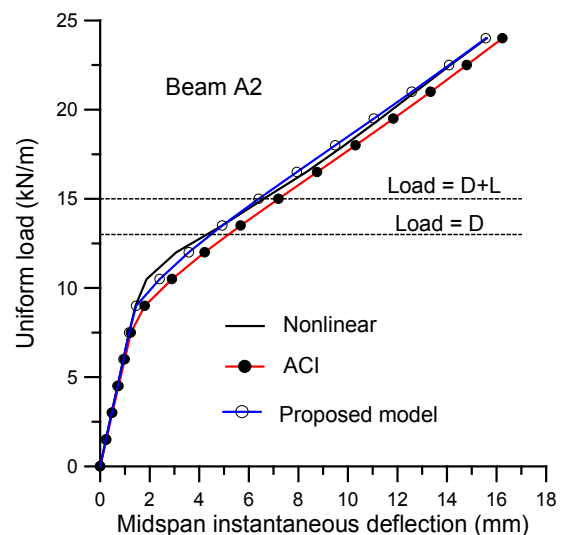


Fig. 9 – Load-instantaneous deflection curves for beam A2

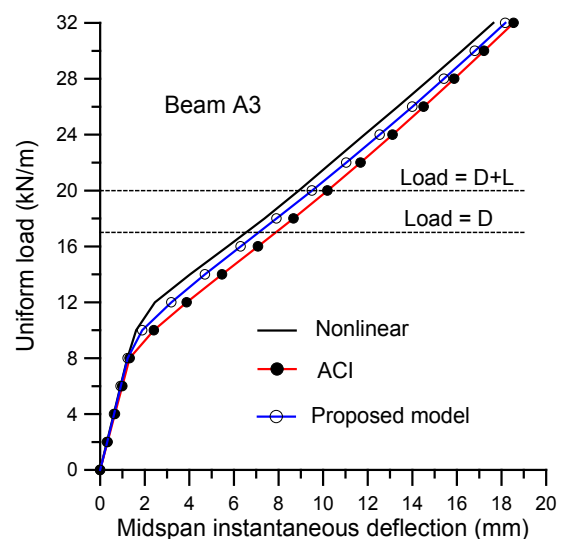


Fig. 10 – Load-instantaneous deflection curves for beam A3

Table 2 – Instantaneous deflection (mm) for the total service load D+L

Beam	Method		
	Nonlinear	ACI	Proposed model
A1	1.8	2.6	2.2
A2	6.6	7.2	6.4
A3	8.9	10.2	9.5

Fig. 11 to 13 show the relationships between the load and the midspan total deflection, including creep and shrinkage effects. For the ACI method, coefficient $\xi = 2.0$ is considered.

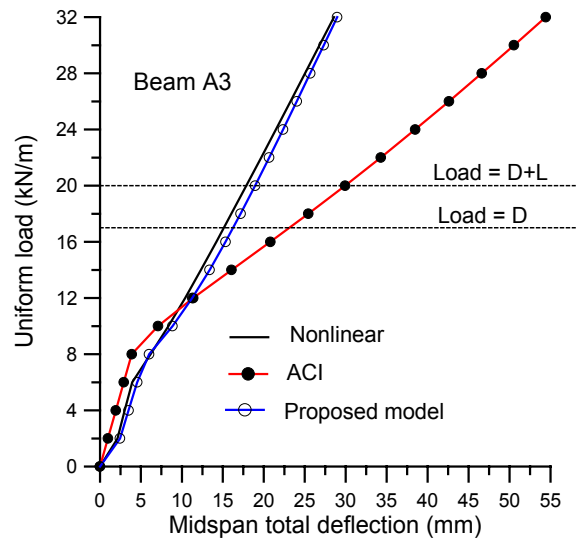


Fig. 13 - Load-total deflection curves for beam A3

As it is observed in Fig. 11 to 13, the proposed model agrees very well with the nonlinear model for all the analyzed beams. This good adjustment is verified in all the levels of loading.

However, the ACI method diverges enough of the nonlinear model. When the load is small and the beam is in the uncracked state, the method of ACI underestimates the total deflection. On the other hand, this method overestimates the total deflections for higher loads. Usually, the total deflection is overestimated for the service loads.

Table 3 indicates the values of total deflection obtained with the three methods for the service load $D+L$. As it is observed, the ACI method overestimates the total deflection, except for the beam A1.

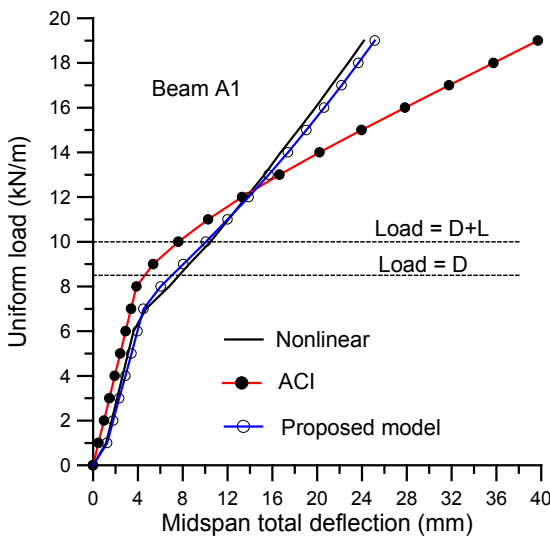


Fig. 11 - Load-total deflection curves for beam A1

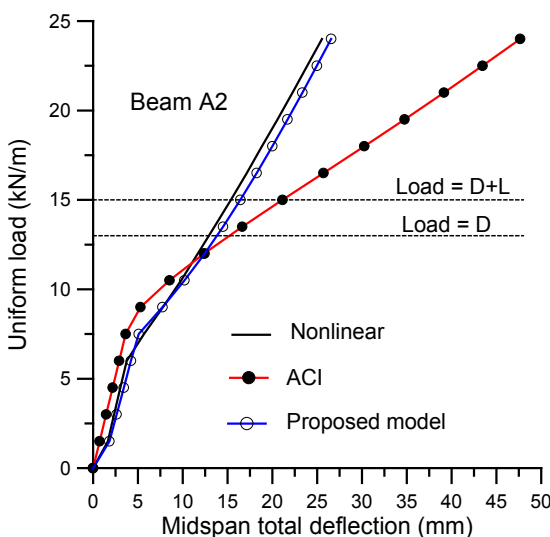


Fig. 12 - Load-total deflection curves for beam A2

Table 3 – Total deflection (mm) for the service load D+L

Beam	Method		
	Nonlinear	ACI	Proposed model
A1	10.5	7.6	10.1
A2	15.4	21.1	16.4
A3	17.9	29.9	18.9

With the values of the Tables 2 and 3, it can be obtained the relationships between the additional deflection ΔW and the instantaneous deflection $W(t_o)$. Those relationships are presented in the Fig. 14.

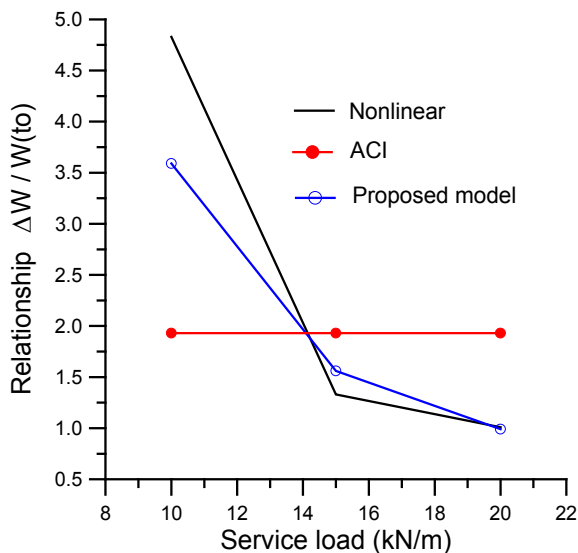


Fig. 14 - Variation of $\Delta W/W(t_0)$ as a function of the load

As it is observed, the relationship $\Delta W/W(t_0)$ depends on the loading level. Then, the expression (11) represents only a rude approach to creep and shrinkage effects in the reinforced concrete beams deflections. That expression was determined empirically, based on a series of experimental results^{21,22}. Consequently, it is only appropriate to reproduce the specific conditions adopted in those tests.

In Fig. 15 the results obtained in 15 single span rectangular beams tested by Washa and Fluck²⁴ are presented. The test data were extracted from Reference [25]. The creep coefficient and shrinkage strain were calculated according to CEB¹, resulting mean values $\varphi = 3,5$ and $\varepsilon_{cs} = -60 \times 10^{-5}$.

As it is observed, the three analyzed methods are satisfactory to reproduce the experimental results with a tolerance of $\pm 20\%$. In this case, the ACI method is also satisfactory, but those beams served as base for attainment of the equation (11). However, this equation cannot be generalized for other test conditions.

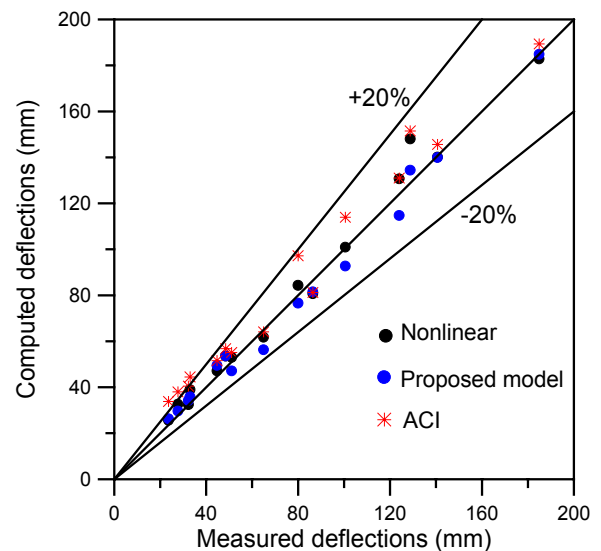


Fig. 15 – Comparison of computed and measured long-time deflections

7. CONCLUSIONS

Based on the results presented, it may be concluded that the method of ACI is satisfactory for the evaluation of instantaneous deflections of reinforced concrete beams. The effective moment of inertia considers the tension stiffening effect in spite of ignoring the contribution of the reinforcement for uncracked sections.

However, the ACI method is not appropriate for evaluation of the total deflections of reinforced concrete beams. When this method is used, the following mistakes are expected:

1. In structural elements that behave in an uncracked state, as solid slabs and beams submitted to loads of small intensity, the effects of the concrete delayed strains (creep and shrinkage) are underestimated. In this case, the design is not reliable in relation to the limit state of deformation.

2. In elements that behave in the cracked state, as most of the beams of buildings, the effects of the concrete delayed strains are overestimated. In this case, the design is anti-economical.

Besides, the expression (11) is independent of the creep coefficient and of the shrinkage strain. That expression was determined empirically, based on a series of experimental results. Consequently, it is only appropriate to reproduce the specific conditions adopted in those tests.

Any general expression for the relationship $\Delta W/W(t_o)$ should take into account the following factors:

- degree of cracking of the beam, measured through the relationship M_r/M ;
- steel rates $\rho = A_s/(bd)$ and $\rho' = A'_s/(bd)$;
- value of the creep coefficient φ ;
- value of the shrinkage strain ε_{cs} .

Consequently, the method of ACI is not very appropriate for calculation of deflections of reinforced concrete beams due to creep and shrinkage of concrete.

The proposed model has the purpose of eliminating the mistakes of the ACI method. As it was shown, it reproduces the results obtained through the nonlinear analysis as well as the experimental results. Besides, the proposed model preserves the simplicity of the ACI method, what facilitates its employment in the structural design.

REFERENCES

1. Comité Euro-International du Béton - *CEB-FIP Model Code 1990*, Thomas Telford, Lausanne, 1993, 437 pp.
2. Comité Euro-International du Béton - *Regles Unifiées Communes aux Différents Types d'Ouvrages et de Matériaux*, V. 1, Paris, 1978, 101 pp. (in French).
3. Comité Euro-International du Béton - *CEB Design Manual on Cracking and Deformations*, Lausanne, 1985.
4. European Committee for Standardization - *Eurocode 2: Design of Concrete Structures. Part 1-1: General Rules and Rules for Buildings*, Final draft, Dec. 2003, 223 pp.
5. American Concrete Institute - *Building Code Requirements for Structural Concrete (ACI 318-95) and Commentary (ACI 318R-95)*, Detroit, 1995, 369 pp.
6. Permanent Commission of Concrete - *Instruction of Structural Concrete*, EHE, Madrid, Spain, 1999, 470 pp. (in Spanish).
7. Brazilian Society of Technical Norms - *Design of Concrete Structures*, NBR-6118, Rio de Janeiro, Brazil, 2004, 221 pp. (in Portuguese).
8. Araújo, J. M. - *A Model for Analysis of Reinforced Concrete Beams*, Portuguese Magazine of Structural Engineering, No. 32, Lisbon, Portugal, 1991, pp. 9-14. (in Portuguese).
9. Gilbert, R. I., and Warner, R. F. - *Tension Stiffening in Reinforced Concrete Slabs*, Journal of the Structural Division, ASCE, V.104, No.12, Dec. 1978, pp. 1885-1900.
10. Vecchio, F. J., and Collins, M. P. - *The Modified Compression Field Theory for Reinforced Concrete Elements Subjected to Shear*, ACI Journal, V. 83, No. 2, March-April 1986, pp. 219-231.
11. Wang, T., and Hsu, T. T. C. - *Nonlinear Finite Element Analysis of Concrete Structures Using New Constitutive Models*, Computers & Structures, V. 79, Dec. 2001, pp. 2781-2791.
12. Cervenka, V., - *Constitutive Model for Cracked Reinforced Concrete*, ACI Journal, V. 82, No. 6, Nov. 1985, pp. 877-882.
13. Bazant, Z. P., and Wu, S. T. - *Rate Type Creep Law of Aging Concrete Based on Maxwell Chain*, Materials and Structures, V. 7, No. 37, 1974, pp. 45-60.
14. Bazant, Z. P., and Prasannan, S. - *Solidification Theory for Concrete Creep. I: Formulation, II: Verification and Application*, Journal of Engineering Mechanics, V. 115, No. 8. Aug. 1989, pp. 1691-1725.
15. Araújo, J. M. - *Nonlinear Analysis of Solid and Ribbed Reinforced Concrete Slabs*, Portuguese Magazine of Structural Engineering, No. 52, Lisbon, Portugal, 2003, pp. 43-52. (in Portuguese).
16. Desayi, K., and Krishnan, S. - *Equation for the Stress-Strain Curve of Concrete*, ACI Journal, V. 61, No. 3, March 1964, pp.345-350.
17. Saenz, L. P. - *Discussion of Equation for the Stress-Strain Curve of Concrete by K. Desayi and S. Krishnan*, ACI Journal, V. 61, No. 9, Sept. 1964, pp. 1229-1235.
18. Ghali, A., and Favre, R. - *Concrete Structures: Stresses and Deformations*, Chapman and Hall, London, 1986, 352 pp.
19. Comité Euro-International du Béton - *CEB Design Manual on Structural Effects of Time-Dependent Behaviour of Concrete*, Switzerland, 1984, 391 pp.
20. Branson, Dan E. - *Instantaneous and Time-Dependent Deflections of Simple and Continuous Reinforced Concrete Beams*, HPR Report No. 7, Part 1, Alabama Highway Department, Bureau of Public Roads, Aug. 1965, 78 pp.
21. Branson, Dan. E. - *Compression Steel Effect on Long-Time Deflections*, ACI Journal, V. 68, No. 8, Aug. 1971, pp. 555-559.

22. Yu, Wei-Wen, and Winter G. - *Instantaneous and Long-Time Deflections of Reinforced Concrete Beams Under Working Loads*, ACI Journal, V. 57, No. 1, July 1960, pp. 29-50.

23. Branson, Dan E., and Trost, H. - *Unified Procedures for Predicting the Deflection and Centroidal Axis Location of Partially Cracked Nonprestressed and Prestressed Concrete Members*, ACI Journal, V. 79, No. 2, March-April 1982, pp. 119-130.

24. Washa, G. W., and Fluck, P. G. - *The Effect of Compressive Reinforcement on the Plastic Flow of Reinforced Concrete Beams*, ACI Journal, V. 49, No. 8, Oct. 1952, pp. 89-108.

25. ACI Committe 435 - *Deflections of Reinforced Concrete Flexural Members*, ACI Journal, V. 63, No. 6, June 1966, pp. 637-674.